Direct observation of the Kr $(3d^{-1}4p^{-1})$ and Xe $(4d^{-1}5p^{-1})$ doubly charged ion states by threshold-photoelectron coincidence spectroscopy

P. Bolognesi and L. Avaldi
CNR-IMAI, Area della Ricerca di Roma, CP10 00016 Monterotondo Scalo, Rome, Italy

M. C. A. Lopes,* G. Dawber, and G. C. King
Department of Physics and Astronomy, Manchester University, M13 9PL Manchester, United Kingdom

M. A. MacDonald
Daresbury Laboratory, Daresbury, Warrington WA4 4AD, United Kingdom

C. Villani and F. Tarantelli
Dipartimento di Chimica, Università di Perugia, 06100 Perugia, Italy
(Received 16 November 2000; published 30 May 2001)

Threshold-photoelectron coincidence spectra and threshold-photoelectron spectra are measured for Kr and Xe in the energy regions 105–127 and 75–100 eV, respectively. Kr^{2+} $3d^{-1}4p^{-1}$ and Xe^{2+} $4d^{-1}5p^{-1}$ doubly charged ion states are observed, and also Kr^{+} $3d^{-1}4p^{-1}nl$ and Xe $4d^{-1}5p^{-1}nl$ satellite states. To our knowledge, this is the first direct observation in electron spectroscopy of doubly charged ion states where one hole occurs in an inner shell and another in a valence shell. The results are compared with theoretical calculations performed with an algebraic Green's-function method, and also with previous experimental information from Auger electron spectroscopy.

DOI: 10.1103/PhysRevA.64.012701 PACS number(s): 32.80.Fb, 32.30.−r

I. INTRODUCTION

Auger electron spectroscopy [1] and optical measurements [2] have for a long time been the main sources of spectroscopic information on doubly charged ions (dications). The optical measurements, from gas discharge experiments are characterized by high resolution, but only provide relative energies with respect to a reference point, which is usually the ground state of the dication. Information from Auger electron spectroscopy is usually limited by the natural width of the inner-shell state and by the energy resolution of the electron spectrometer. It also relies on the accuracy of the known values of the inner-shell ionization potentials. A direct approach to the spectroscopy of atomic dications can be achieved via photodouble ionization experiments, where the two photoelectrons are detected in coincidence. The most efficient among these is the threshold-photoelectron–threshold-photoelectron coincidence (TPEsCO) technique, because it deals with low-energy photoelectrons that can be collected with high-energy resolution and efficiency [3]. Since its introduction, the TPEsCO technique has been successfully employed to study the lowest-lying dication states of rare gases [4–6], diatomic molecules [3,7,8], and polyatomic molecules [9]. These studies have also been extended to excited states of dications in Ne, Ar [10,11], and Xe [12]. In the present work we have used the TPEsCO technique to make a study of dication states where there is a hole in an inner-shell orbital and one in a valence orbital, namely, $Kr^{2+}(3d^{-1}4p^{-1})$ and Xe^{2+} $(4d^{-1}5p^{-1})$. Direct photodouble ionization occurs only because of correlations between the target electrons. In the present case the electrons involved are in different shells; thus this study provides information on ''intershell'' correlations.

In the interpretation of our coincidence spectra we have been aided by previous Kr $M_{2,3}M_{4,5}N_{2,3}$ Coster-Kronig [13] and Xe $M_{4,5}N_{4,5}O_{2,3}$ Auger measurements [14]. In order to confirm this interpretation, we have carried out *ab initio*, post-Hartree-Fock calculations on the double-ionization spectra of Kr and Xe. For this we have used the algebraic diagrammatic construction [ADO(2)] method in second-order perturbation theory based on Green's functions [15]. Previously this method was used successfully for an accurate simulation of the Auger spectra of many molecular systems [16], and also for an interpretation of molecular double-charge-transfer spectra [17]. In a somewhat closer connection to the present experiments, the ADC(2) method was also used to predict and interpret double-ionization processes involving one core electron and one valence electron [18]. The ADC(2) method is based on a matrix representation of the particle-particle propagator in the space of the final Hartree-Fock di-cation states. The eigenvalues directly provide the double-ionization energies of the system. The computed energies of the ''main'' states, which are derived from two-hole $(2h)$ configurations (i.e., the neutral Hartree-Fock configurations without two electrons) are correct to second-order perturbation theory. The energies of ''satellite'' states which involve a single excitation of the $2h$ states are correct only to first order. The ADC eigenvectors provide correspondingly accurate spectroscopic factors, i.e., relative intensities of the different states.

II. EXPERIMENT

The experiment was performed at the TGM beamline of the Daresbury Synchrotron Radiation Source. The threshold

*Permanent address: Departamento de Fisica, ICE, Universidade Federal de Juiz de Fora, MG, CEP:36030-330, Brazil.

coincidence spectrometer and its modes of operation were described in detail elsewhere [19,3]. Briefly, it consists of an effusive gas beam and two identical electron energy analyzers [20], which use a penetrating field technique [21] for the efficient collection of nearly zero energy (threshold) electrons. In the TPEsCO mode of operation of the spectrometer, coincidences between the threshold electrons detected in the two analyzers are measured as the photon energy is scanned across the region of interest. Simultaneously with this TPEsCO measurement, the yields of threshold photoelectrons from each single analyzer are recorded to give the threshold photoelectron (TPES) spectrum. The photon energy scale was calibrated by recording the TPES spectrum in the energy region of the Kr $3d^{-1}nl$ states [22]. These highly excited, neutral states lie in both the double- and triple-ionization continua. They can decay to these continua with the emission of two or three electrons, respectively, which can share the excess energy in a continuous manner. Thus, in a constant electron energy spectrum such as a TPES spectrum, they give rise to peaks occurring at the spectroscopic energies of the $3d^{-1}nl$ Rydberg states [23].

III. RESULTS AND DISCUSSION

The TPEsCO spectra obtained in the energy regions 105–127 eV for Kr and 75–100 eV for Xe are shown in Fig. 1. This figure also shows the TPES spectra. For both atoms the TPES spectra show series of peaks corresponding to the excitation of the $(n'd^{-1}n''p^{-1})nl$ satellite states converging to the $(n'd^{-1}n''p^{-1})$ manifold, where $n'=3$ and 4 and $n''=4$ and 5 for Kr and Xe, respectively. A striking feature of the results is the strong resemblance between the TPEsCO and TPES spectra below this manifold.

Satellite states corresponding to $(n'd^{-1}n''p^{-1})np$ transitions were first observed in x-ray photoemission spectroscopy (XPS) measurements [24,25]. Subsequently, TPES measurements [26] revealed the full richness of the spectrum, with the additional observation of peaks due to $(n'd^{-1}n''p^{-1})ns$ and nd conjugate shake-up transitions, which have cross sections that increase as the threshold is approached. These previous measurements were able to resolve and assign the $(n'd^{-1}n''p^{-1})nl$ satellite states with n up to 7 and 8 in Kr and Xe, respectively. The features in our TPES spectra (Fig. 1) have been labeled $A-F$ according to the notation of Ref. [26]. The present experiment has better energy resolution and counting statistics than the previous work. This has allowed the splitting of peaks A and E, and the observation of interesting features above the F peaks. More than 36 series are expected for the $(n'd^{-1}n''p^{-1})nl$ satellite states [25] and this prevents a precise assignment of the different peaks that contribute to the A and E features. The features above the F peaks can be assigned to higher-n members of the $(n'd^{-1}n''p^{-1})nl$ series, and to the first terms of the series of the $(n'd^{-1}n''s^{-1})nl$ satellite states. An example of the latter is represented by the small features at about 96 eV in the Xe spectrum that have been assigned to the $(4d^{-1}5s^{-1})6s$ state in XPS measurements [25].

As noted above the TPEsCO spectra in the energy region of the $A-F$ peaks mimic the structures in the TPES spectra.

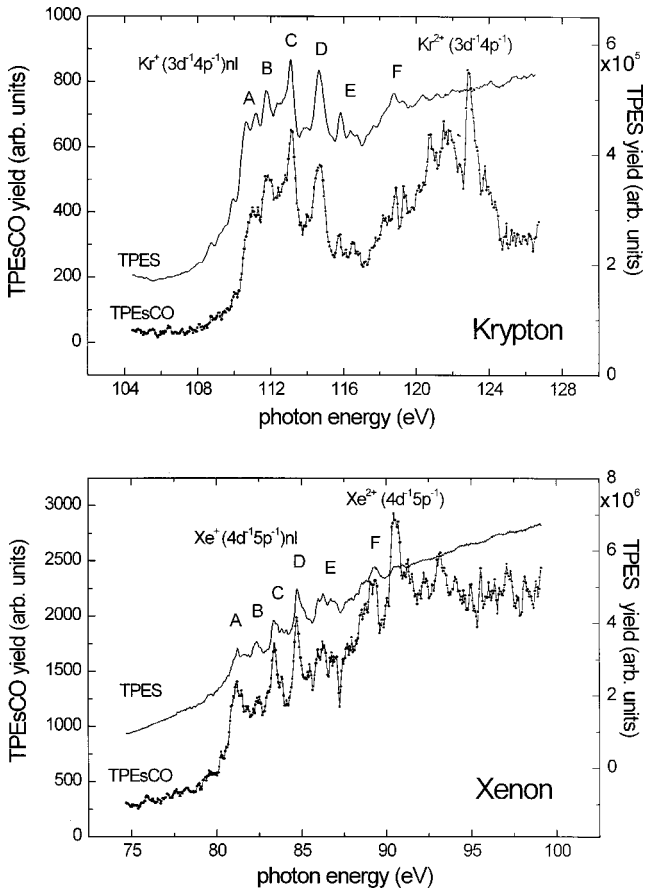

FIG. 1. TPES (solid line) and TPEsCO (dots) spectra of Kr (top panel) and Xe (bottom panel) in the region of the $(n'd^{-1}n''p^{-1})$ di-cation states, where $n'=3$ and 4 and $n''=4$ and 5 for Kr and Xe, respectively. The $(n'd^{-1}n''p^{-1})nl$ satellite states have been labeled $A-F$ according to the notation from Ref. [26]. Typical count rates and true to random ratios are typically 2.5 Hz and 1.5/1 in Kr and 12 Hz and 1/5 in Xe. The statistical uncertainty is about 10% of the coincidence counts.

This observation is explained by the fact that the $(n'd^{-1}n''p^{-1})nl$ states are embedded in the doubly and triply charged ion continua (see Fig. 2 for the case of Kr). They preferentially decay to the latter with the ejection of two electrons. This has been proved by the observations of the threshold-photoelectron–photoion-coincident (TPEPICO) measurements of Hayaishi *et al.* [27]. That experiment showed that decay to the triply charged ions is the dominant channel. The coincidence yield for this channel displayed a broad band in the region above the $n'd^{-1}$ thresholds, and changes in the slopes at about 110 and 82 eV in Kr and Xe, respectively. The broad band was interpreted as the formation of triply charged ions via double Auger decay of the $n'd^{-1}$ hole, while the changes in the slopes were attributed to the formation and decay of $(n'd^{-1}n''p^{-1})nl$ satellite states. In a TPEsCO experiment two correlated, threshold electrons are detected in coincidence, and for the present measurements we propose the following origins of these electrons. The first arises from the photoionization of the satellite state at its threshold. The second may be produced either in a subsequent double-Auger decay for the extreme

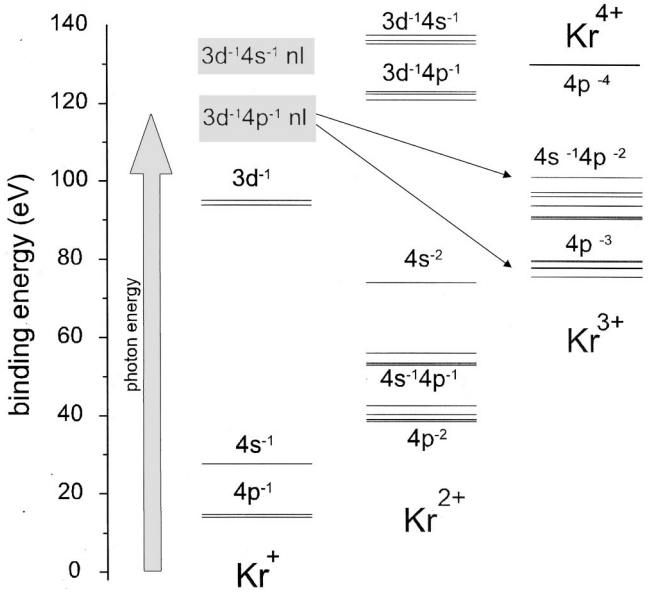

FIG. 2. Schematic energy diagram of Kr.

energy sharing condition, i.e., where one electron has zero energy, e.g.,

$$h\nu + \mathrm{Kr} \rightarrow \mathrm{Kr}^{+}(3d^{-1}4p^{-1}nl) + e^{-}(E \sim 0\ \mathrm{eV}),$$
$$\downarrow \tag{1a}$$
$$\mathrm{Kr}^{3+} + e^{-}(E_a) + e^{-}(E \sim 0\ \mathrm{eV}),$$

where $E_a = E_{\mathrm{bin}}(\mathrm{Kr}^{+}3d^{-1}4p^{-1}nl) - E_{\mathrm{bin}}(\mathrm{Kr}^{3+})$;
or in the decay to an excited state of the doubly charged ion, which is accidentally degenerate with a triply charged ion state, e.g.,

$$h\nu + \mathrm{Kr} \rightarrow \mathrm{Kr}^{+}(3d^{-1}4p^{-1}nl) + e^{-}(E \sim 0\ \mathrm{eV})$$
$$\downarrow \tag{1b}$$
$$\mathrm{Kr}^{2+} + e^{-}(E_a)$$
$$\downarrow$$
$$\mathrm{Kr}^{3+} + e^{-}(E \sim 0\ \mathrm{eV})$$

where $E_a = E_{\mathrm{bin}}(\mathrm{Kr}^{+}3d^{-}4p^{-1}nl) - E_{\mathrm{bin}}(\mathrm{Kr}^{2+})$.
Thus the replication of the satellite structure in the TPEsCO spectrum clearly confirms the relevance of the decay of the satellite states to the triply charged ion continuum.

It is also interesting to observe that peaks due to the satellite states occur at the same energy, within the energy resolution of the measurements, in the TPES and TPEsCO spectra. It is well known that in the nonradiative decay of an inner-shell hole there is Coulomb interaction between the outgoing charged particles known as post-collision interaction (PCI). This results in a shifting of peaks and a broadening of their line shapes. The TPES measurement is not selective in the decay channel. Thus the peaks observed in the TPES spectra may be affected by PCI effects from many possible allowed decay channels. On the other hand, the peaks in the TPEsCO spectra are only affected by the PCI effect due to the channels represented in Eqs. (1). Therefore, the observation that the satellite peaks occur at the same energy in the TPES and TPEsCO spectra suggests that the extreme energy sharing decay route is the dominant one as far as PCI effects are concerned.

Above the peaks labeled *F* in Fig. 1, i.e., in the energy region approaching the limit of the satellite series, the density of states is such that the features become indistinguishable in the TPES spectrum. On the other hand, well-defined peaks are observed in the TPEsCO spectra in the energy regions 120–125 eV in Kr and 90–95 eV in Xe (Fig. 1). These peaks are mainly attributed to direct double ionization the $\mathrm{Kr}^{2+}(3d^{-1}4p^{-1})$ and $\mathrm{Xe}^{2+}(4d^{-1}5p^{-1})$ manifolds. They are superimposed on the triple-ionization continuum, that has contributions from the direct triple-ionization process, from the decay of the Kr^{2+} states accidentally degenerate with a Kr^{2+} state and from the decay of the $\mathrm{Kr}^{+}\ 3d^{1}$ and $\mathrm{Xe}^{+}\ 4d^{-1}$ states (Fig. 2). The last contribution is expected to be the dominant one, due to the giant resonances observed in the $\mathrm{Kr}^{+}(3d^{-1})$ and $\mathrm{Xe}^{+}(4d^{-1})$ cross sections in the energy regions investigated. This is confirmed by the observation of the almost vanishing TPEsCO yield in the lowest-energy part of the spectra of Fig. 1, i.e., in the region where the $\mathrm{Kr}^{+}(3d^{-1})$ and $\mathrm{Xe}^{+}(4d^{-1})$ cross sections are not yet affected by the resonance. Based on this observation we have deduced the shape of the contribution of the triple ionization to the TPEsCO spectra by fitting a polynomial function to the Kr^{3+} and Xe^{3+} TPEPICO spectra of Hayaishi *et al.* [27], that in the region of interest are also dominated by the *d* cross sections. The TPEsCO spectra for the inner-valence dication states of Kr and Xe, after the subtraction of the triple-ionization contribution, are shown in greater detail in the bottom panels of Figs. 3(a) and 3(b), respectively. The TPEsCO spectra may contain additional contributions from higher members of the $(n'd^{-1}n''p^{-1})nl$ ($n \geqslant 7$ and 8 in Kr and Xe, respectively) satellite states and, in the case of Xe, the first terms of the $(n'd^{-1}n''s^{-1})nl$ ($n \geqslant 6$) satellite states.

Despite the fact that the Kr and Xe $(n'd^{-1}n''p^{-1})$ states are expected to be close to the *jj*-coupling limit, all previous studies have used an *LS* description. In *LS* coupling, 12 different terms with the configurations $^{1}D_2$, $^{3}D_{1,2,3}$, $^{3}F_{2,3,4}$, $^{3}P_{0,1,2}$, $^{1}F_3$, and $^{1}P_1$, contribute to the $(n'd^{-1}n''p^{-1})$ manifold. Spectroscopic information on these inner-valence dication states can be obtained in an indirect way via Auger measurements. For example, the energies of the $(n'd^{-1}n''p^{-1})$ states can be derived from the Kr $M_{2,3}M_{4,5}N_{2,3}$ [13] Coster-Kronig and Xe $M_{4,5}N_{4,5}O_{2,3}$ [14] Auger measurements using Kr $3p$ and Xe $3d$ ionization potentials [28,29]. Kr $M_{4,5}N_{2,3}$-$N_{2,3}N_{2,3}N_{2,3}$ and Xe $N_{4,5}O_{2,3}$-$O_{2,3}O_{2,3}O_{2,3}$ satellite Auger spectra [30], which correspond to transitions from the $n'd^{-1}n''p^{-1}$ states to the $n''p^{-3}$ triply charged ion, might also be used. However this second approach suffers from a large uncertainty in the known potentials for triple ionization. For example, the experimental values of Dorman and Morrison [31] differ by 2.1 and 0.7 eV in Kr and Xe, respectively from the ones obtained using Moore's tables [32], and so this approach has not been

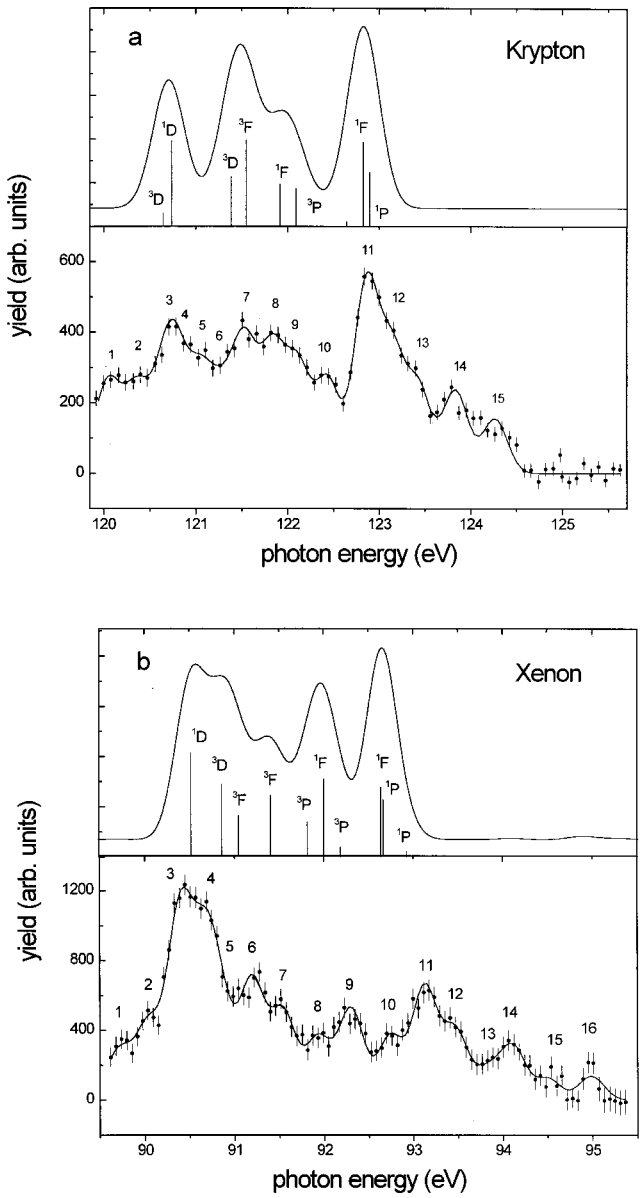

FIG. 3. Region of the Kr^{2+} (a) and Xe^{2+} (b) inner-valence dication states. In the bottom panels the experimental spectra after the subtraction of the continuum due to triple ionization are shown. The full line is a fit to the experimental data with a set of Gaussian functions (see Tables I and II for Kr and Xe, respectively). In the top panels the theoretical spectra computed with the ADC(2) method and convoluted with the experimental resolution are shown.

used. Additional information on the relative energies of the different configurations and the spin-orbit splittings can be extracted from calculations performed for the $(n'd^{-1}n''p^{-1})np$ satellite states (see Tables 11 and 17 of Ref. [25] for Kr and Xe, respectively) and the Kr $M_{4,5}N_{2,3}$-$N_{2,3}N_{2,3}N_{2,3}$ and Xe $N_{4,5}O_{2,3}$-$O_{2,3}O_{2,3}O_{2,3}$ satellite Auger transitions (see Tables I and II of Ref. [24]).

Using these earlier measurements as a starting point, a series of Gaussian functions of fixed full width at half maximum (FWHM) has been fitted to the experimental data. The chosen values for the FWHM were 310 meV in Kr and 330 meV in Xe. These values result from the natural widths of the dication states that are assumed to be equal to the *d*-hole widths, convoluted with the apparatus resolution. The results of this fitting procedure are shown in the bottom panels of Figs. 3(a) and 3(b), where the solid continuous lines correspond to the sum of the Gaussian functions. Note that the relative heights of these Gaussians cannot be used for a direct comparison with Auger intensities or calculated intensities, because both direct and indirect processes contribute to the intensities observed in the TPEsCO spectra.

In Tables I and II the deduced energies of the different states are compared with the values derived from the Kr $M_{2,3}M_{4,5}N_{2,3}$ Coster-Kronig and Xe $M_{4,5}N_{4,5}O_{2,3}$ Auger measurements [13,14] and good agreement is observed. In comparing these energy values, account has to be taken of the fact that the present results have not been corrected for any PCI effects. Unfortunately, no previous experimental observations of these effects exist, and the most widely used theory of PCI [33] does not account for the threshold region. However, the magnitude of the energy shift can be roughly estimated assuming that the dominant contribution comes from the natural width of the *d* inner hole. This hypothesis is supported by the observation that satellite Auger peaks [30] do not appear to be broader than the Kr $M_{4,5}N_{23}N_{23}$ and Xe $N_{4,5}O_{23}O_{23}$ lines. In a TPES experiment, Avaldi *et al.* [10] measured the PCI shift associated with the $Kr^+ 3d^{-1}$ and $Xe^+ 4d^{-1}$ states to be approximately +200 meV. A similar shift may also be attributed to the energies reported in Tables I and II.

Our proposed assignments of the different spin-orbit configurations are based on a comparison with the core configurations of the $n'd^{-1}n''p^{-1}(^{2S+1}L_J)5p$ and $6p$ satellite states in Kr and Xe, respectively, given by Svensson *et al.* [25]. At variance with that assignment, here we have exchanged the $^3F_2$ and $^3P_2$ states to be consistent with the assignment proposed for the Kr $M_{2,3}M_{4,5}N_{2,3}$ Coster-Kronig and Xe $M_{4,5}N_{4,5}O_{2,3}$ Auger measurements [13,14]. The extra features needed to improve the fit of the measured spectrum may be assigned to Kr^+ and Xe^+ satellite states (see Tables I and II). This conclusion is supported by the good match of some of these features with the previous XPS and TP measurements [25,26].

We now turn to a discussion of the spectra in the light of the Green's-function calculations. The Hartree-Fock calculations on the neutral closed-shells of Kr and Xe were performed with the GAMESS-UK package [34] using a contracted Gaussian cc-pVTZ basis set [35] and a decontracted Gaussian DZVP [36] for Kr and Xe, respectively. Decontraction of the Xe basis was adopted to allow for greater flexibility in the description of the dicationic state manifold. In the theoretical simulation of the double-ionization spectra of heavy atoms, both relativistic effects and electron correlation play important roles and need to be accounted for. This is, however, very difficult to achieve. The relativistic effects in the ground state of the atoms and in the orbital basis have been accounted for by the introduction of a relativistic ZORA potential [37] in the Hatree-Fock calculation. On the other hand, the Green's-function method we have used neglects spin-orbit coupling effects in the final-state manifold, and

TABLE I. Experimental energies for the $Kr^{2+}(3d^{-1}4p^{-1})$ states as obtained from a fit to the present TPEsCO data in Fig. 3(a). These results are compared with previous Auger measurements [13], whose assignments are followed in the table. For the M_2 initial hole a binding energy of 222.2 eV has been used [28]. The labels in the last column refer to the bar diagram in Fig. 3(a).

Reference [13]		This work		
Assignment $Kr^{2+}(3d^{-1}4p^{-1})$	Energies	Assignment	Energies	Peak label
		$Kr^{+}(3d^{-1}4p^{-1}7s7p)$	120.04±0.10	1
		$Kr^{+}(3d^{-1}4p^{-1}7s/7p)$[a]	120.36±0.10	2
		$^1D_2$	120.68±0.20	3
$(^1D_2, {}^3D_3, {}^3F_4,)$	120.89	$Kr^{+}(3d^{-1}4p^{-1}7p)$	120.82±0.10	4
		$^3D_3$	121.05±0.10	5
		$^3F_4$	121.28±0.20	6
$(^3D_1, {}^3D_2, {}^3F_3)$	121.72	$Kr^{+}(3d^{-1}4p^{-1}7p)$[a]	121.53±0.20	7
		$^3D_2, {}^3D_1$	121.83±0.30	8
		$^3F_3$	122.11±0.40	9
$(^3P_2, {}^3P_1)$	122.25	$^3P_2, {}^3P_1$	122.44±0.20	10
		$^3P_0$	122.86±0.10	11
$(^3P_0, {}^3F_2, {}^1F_3)$	122.88	$^3F_2$	123.14±0.10	12
		$^1F_3$	123.43±0.20	13
$^1P_1$	124.04	$^1P_1$	123.85±0.20	14
			124.26±0.10	15

[a]Reference [25].

TABLE II. Experimental energies for the $Xe^{2+}(4d^{-1}5p^{-1})$ states as obtained from a fit to the present TPEsCO data in Fig. 3(b). These results are compared with previous Auger measurements of Ref. [14], whose assignments are followed in the table. For the $M_{4,5}$ initial holes, binding energies of 676.7 and 689.4 eV, respectively, have been used [29]. The labels in the last column refer to the bar diagram in Fig. 3(b).

Ref. [14]			This work		
Assignment	Energies				
$Xe^{2+}(4d^{-1}5p^{-1})$	M_4	M_5	Assignment	Energies	Peak label
			$Xe^{+}(4d^{-1}5p^{-1}8s/8p)$[a]	89.71±0.10	1
			$Xe^{+}(4d^{-1}5p^{-1}8s/8p)$[a]	90.04±0.10	2
$(^1D_2, {}^3D_3, {}^3F_3,)$		90.40	$^1D_2$	90.39±0.20	3
			$^3D_3$	90.67±0.14	4
			$^3F_4$	90.86±0.10	5
$(^3D_1)$	91.50	91.33	$^3D_1$	91.19±0.05	6
				91.54±0.06	7
$(^3D_2, {}^3F_3)$,	92.10	92.17	$^3D_2$ or	91.93±0.04	8
			$Xe^{+}(4d^{-1}5p^{-1}8p)$[b] $^3F_3$	92.30±0.03	9
$(^3P_2, {}^3P_1)$	92.60		$^3P_2, {}^3P_1$	92.74±0.05	10
$(^3P_0, {}^1F_3)$	93.00	93.00	$^3P_0$	93.12±0.05	11
			$^1F_3$	93.47±0.09	12
				93.83±0.20	13
$(^3F_2)$	93.93		$^3F_2$	94.11±0.20	14
			$Xe^{+}(4d^{-1}5s^{-1}6s)$[b]	94.50±0.21	15
$(^1P_1)$	94.71		$^1P_1$	94.98±0.06	16

[a]Reference [26].
[b]Reference [25].

thus cannot provide a truly quantitative description. The method accurately accounts for electron correlation effects, treating them uniformly throughout the spectrum of dication states and balancing implicitly ground-state and final-state descriptions. Another advantage of this method is that it directly reproduces the full ionization spectrum, avoiding the calculation of individual correlated states that are unknown *a priori*.

The calculated double-ionization spectra in the energy region of interest are displayed in the top panels of Figs. 3(a) and 3(b). These spectra were obtained by a Gaussian convolution of the computed transitions, using a FWHM of 0.4 eV for each Gaussian, and the $2h$ spectroscopic factors as relative intensities. This provides only a useful estimate of the true intensities since the calculation of accurate transition rates is a very difficult problem. However this approximation has generally been found to be quite satisfactory in the study of Auger spectra [15]. Also, in the present case, it is reasonable to expect the final states to be populated from the ground state roughly in proportion to their Hartree-Fock ''main'' character. The theoretical spectra have been shifted to higher energy by 1.1 and 1.2 eV for Kr and Xe, respectively, in order to align them with the principal experimental bands. Such shifts have systematically been encountered in the theoretical study of Auger spectra by the ADC method. This can be attributed to the underestimation of the correlation energy of the ground state that has two more electrons than the final state.

Comparison of the computed and experimental spectra appears to confirm the proposed interpretation of the experimental data, notwithstanding the approximations discussed above. The overall appearance of the spectra and the main peak shapes are reproduced quite satisfactorily by the theory. As expected, electron correlation effects appear to be quite significant, as demonstrated by the appearance in the computed spectra of a larger number of states than would be expected in pure *LS* coupling. In the case of Xe, for example, two *F* triplets, two *F* singlets, two *P* triplets, and two *P* singlets are obtained. However, we note that several weaker features are absent in the calculated spectra, and that the spectral energy span is smaller. Also the relative intensity of some bands (most notably the high energy peak in the Xe spectrum) is estimated to be substantially larger than observed. The origin of these discrepancies lies mostly in the lack of final-state spin-orbit coupling in our calculations. This would cause the intensity of most states to be redistributed over a larger number of lines and over a wider energy span.

In conclusion, the spectra of doubly charged atoms with one hole in an inner shell and one in the valence shell have been measured directly via coincidence electron spectroscopy. The calculations support the assignment of the TPEsCO lines to $n'd^{-1}n''p^{-1}$ states of the atomic dications.

ACKNOWLEDGMENTS

One of us (M.C.A.L.) gratefully acknowledges support from Conselho National de Desenvolvimento Cientifico e Tecnologico—CNPq.

[1] M. Thompson, M. A. Baker, A. Christie, and J. F. Tyson, *Auger Electron Spectroscopy* (Wiley, New York, 1985).
[2] L. Minnhagen, Phys. Scr. **11**, 38 (1975); M. Gallardo, F. Bredice, M. Raineri, and J. Reyna Almandos, Appl. Opt. **28**, 4513 (1989).
[3] R. I. Hall, G. Dawber, A. G. McConkey, M. A. MacDonald, and G. C. King, Phys. Rev. Lett. **68**, 2751 (1992).
[4] R. I. Hall, G. Dawber, A. G. McConkey, M. A. MacDonald, and G. C. King, Z. Phys. D: At., Mol. Clusters **23**, 377 (1992).
[5] R. I. Hall, G. Dawber, A. G. McConkey, M. A. MacDonald, and G. C. King, J. Phys. B **25**, 377 (1992).
[6] B. Krässig and V. Schmidt, J. Phys. B **22**, L153 (1992).
[7] A. G. McConkey, G. Dawber, L. Avaldi, M. A. MacDonald, G. C. King, and R. I. Hall, J. Phys. B **27**, 271 (1994).
[8] G. Dawber, A. G. McConkey, L. Avaldi, M. A. MacDonald, G. C. King, and R. I. Hall, J. Phys. B **27**, 2191 (1994).
[9] R. I. Hall, L. Avaldi, G. Dawber, A. G. McConkey, M. A. MacDonald, and G. C. King, Chem. Phys. **187**, 125 (1994).
[10] L. Avaldi, R. I. Hall, G. Dawber, P. M. Rutter, and G. C. King, J. Phys. B **24**, 427 (1991).
[11] L. Avaldi, G. Dawber, G. C. King, G. Stefani, and M. Zitnik, Phys. Rev. A **52**, R3409 (1995).
[12] P. Bolognesi, S. J. Cavanagh, L. Avaldi, R. Camilloni, M. Zitnik, M. Stuhec, and G. C. King, J. Phys. B **33**, 4723 (2000).
[13] J. Jauhiainen, A. Kivimäki, S. Aksela, O.-P. Sairanen, and H. Aksela, J. Phys. B **28**, 4091 (1995).
[14] A. Kivimäki, H. Aksela, J. Jauhiainen, M. Kivilompolo, E. Nömmiste, and S. Aksela, J. Electron Spectrosc. Relat. Phenom. **93**, 89 (1998).
[15] J. Schirmer and A. Barth, Z. Phys. A **317**, 267 (1984).
[16] F. Tarantelli, L. S. Cederbaum, and A. Sgamellotti, J. Electron Spectrosc. Relat. Phenom. **76**, 47 (1995).
[17] R. P. Grant, F. M. Harris, and D. E. Parry, Int. J. Mass Spectrom. Ion Processes **85**, 651 (1999).
[18] H. D. Schulte, L. S. Cederbaum, and F. Tarantelli, Phys. Rev. A **60**, 2047 (1999); H. D. Schulte, L. S. Cederbaum, and F. Tarantelli, J. Chem. Phys. **105**, 108 (1996).
[19] R. I. Hall, A. G. McConkey, K. Ellis, G. Dawber, L. Avaldi, M. A. MacDonald, and G. C. King, Meas. Sci. Technol. **3**, 316 (1992).
[20] G. C. King, M. Zubek, P. M. Rutter, and F. H. Read, J. Phys. E **20**, 440 (1987).
[21] S. Cvejanovic and F. H. Read, J. Phys. B **7**, 118 (1974).
[22] G. C. King, M. Tronc, F. A. Read, and R. C. Bradford, J. Phys. B **10**, 2479 (1977).
[23] L. Avaldi, R. I. Hall, G. Dawber, P. M. Rutter, and G. C. King, J. Phys. B **24**, 427 (1991).
[24] D. J. Bristow, L. S. Tse, and G. M. Bancroft, Phys. Rev. A **25**, 1 (1982).
[25] S. Svensson, B. Eriksson, N. Mårtensson, G. Wendin, and U.

Gelius, J. Electron Spectrosc. Relat. Phenom. **47**, 327 (1988).
[26] T. Hayaishi, E. Murakami, Y. Morioka, H. Aksela, S. Aksela, E. Shigemasa, and A. Yagishita, Phys. Rev. A **44**, R2771 (1991).
[27] T. Hayaishi, A. Yagishita, E. Shigemasa, E. Murakami, and Y. Morioka, Phys. Scr. **41**, 35 (1990).
[28] K. Siegbahn, C. Nordling, G. Johansson, J. Hedman, P. F. Heden, K. Hamrin, U. Gelius, T. Bergmark, L. O. Werme, R. Manne, and Y. Baer, *ESCA Applied to Free Molecules* (North-Holland, Amsterdam, 1969).
[29] O. Yagci and J. E. Wilson, J. Phys. C **16**, 383 (1983).
[30] A. Kivimäki, H. Aksela, J. Jauhiaien, A. Naves de Brito, O.-P. Sairanen, and S. Aksela, Phys. Rev. A **49**, 5124 (1994).
[31] F. H. Dorman and J. D. Morrison, J. Chem. Phys. **34**, 1407 (1961).
[32] C. E. Moore, *Atomic Energy Levels*, Natl. Bus. Stand. Ref. Data Sec., (Natl. Bur. Stand. U.S.) Circ. No. 467 (U.S. GPO, Washington, D.C., 1971), Vol. 35.
[33] M. Y. Kuchiev and S. A. Sheinerman, Zh. Eksp. Teor. Fiz. **90**, 1680 (1986) [Sov. Phys. JETP **63**, 986 (1986)].
[34] GAMESS-UK is a package of *ab initio* programs written by M. F. Guest *et al.*, derived from the original GAMESS code due to M. Dupuis *et al.*, NRCC Software Catalog, Vol. 1, Program No. QG01 (GAMESS), 1980.
[35] D. E. Woon and T. H. Dunning, Jr., J. Chem. Phys. **98**, 1358 (1993).
[36] N. Godbout, D. R. Salahub, J. Andzelm, and E. Wimmer, Can. J. Chem. **70**, 560 (1992).
[37] S. Faas, J. G. Snijders, and J. H. van Lenthe, Prog. Theor. Chem. Phys. **2**, 251 (2000).